

## SUPPLEMENTARY INFORMATION

### **Modelling of green biocatalytic (*R*)-(+)-limonene oxidation using the mycelium of psychrophilic *Cladosporium cladosporioides* 01**

Mateusz Kutyla,<sup>a</sup> Edward Kozłowski,<sup>b</sup> Marek Stankevič,<sup>c</sup> Agnieszka Świca,<sup>a</sup> Mariusz Trytek\*<sup>a</sup>

<sup>a</sup>Department of Industrial and Environmental Microbiology, Faculty of Biology and Biotechnology, Institute of Biological Sciences, Maria Curie-Skłodowska University, Akademicka 19, 20-033, Lublin, Poland. E-mail: mariusz.trytek@mail.umcs.pl

<sup>b</sup>Department of Quantitative Methods in Management, Faculty of Management, Lublin University of Technology, Nadbystrzycka 38, 20-618, Lublin, Poland.

<sup>c</sup>Department of Organic Chemistry and Crystallochemistry, Institute of Chemical Sciences, Maria Curie-Skłodowska University, Gliniana 33, 20-613, Lublin, Poland.

### Estimation of the structural parameters

To estimate the parameters  $\beta \in \mathbb{R}^{1+k(k+1)/2}$  in equation (3)

$$\beta^T = [\beta_0, \beta_1, \beta_2, \dots, \beta_k, \beta_{11}, \dots, \beta_{kk}, \beta_{12}, \dots, \beta_{k-1,k}]$$

the Least Squares Method is used. To this end, the following matrix  $\Pi \in \mathbb{R}^{n \times (1+k(k+1)/2)}$  is defined:

$$\Pi = \begin{bmatrix} 1 & \eta_{11} & \eta_{12} & \dots & \eta_{1k} & \eta_{11}^2 & \dots & \eta_{1k}^2 & \eta_{11}\eta_{12} & \dots & \eta_{1,k-1}\eta_{1,k} \\ 1 & \eta_{21} & \eta_{22} & \dots & \eta_{2k} & \eta_{21}^2 & \dots & \eta_{2k}^2 & \eta_{21}\eta_{22} & \dots & \eta_{2,k-1}\eta_{2,k} \\ \vdots & \vdots & \vdots & \vdots & \vdots & \vdots & \vdots & \vdots & \vdots & \vdots & \vdots \\ 1 & \eta_{n1} & \eta_{n2} & \dots & \eta_{nk} & \eta_{n1}^2 & \dots & \eta_{nk}^2 & \eta_{n1}\eta_{n2} & \dots & \eta_{n,k-1}\eta_{n,k} \end{bmatrix}$$

and the values of the structural parameters  $\beta$  in the equation are determined as follows: if  $\det(\Pi^T \Pi) \neq 0$ , the structural parameter estimators are estimated as follows:

$$\hat{\beta} = (\Pi^T \Pi)^{-1} \Pi^T Y \quad (28)$$

The vector of differences between the empirical values of the endogenous variable and the expected (projected) values are determined as follows

$$\varepsilon = Y - \Pi \hat{\beta} \quad (29)$$

where  $\varepsilon \in \mathbb{R}^n$ . To answer the question of whether model (3) (or model (4)) sufficiently explains the relationship between the endogenous variable and the transformed variables, the coefficient of determination  $R^2$  is estimated

$$R^2 = 1 - \frac{\sum_{i=1}^n \varepsilon_i^2}{\sum_{i=1}^n (y_i - \bar{y})^2} \quad (30)$$

which shows what part of the total variability of the endogenous variable is explained by the transformed variables, where  $\bar{Y} = \frac{1}{n} \sum_{i=1}^n y_i$ . The closer  $R^2$  is to 1, the better the fit of the model.

### Verification of the multiple correlation coefficient

At the significance level  $0 < \alpha < 1$ , a null hypothesis  $H_0: R = 0$  is formed against the alternative hypothesis  $H_1: R \neq 0$ . To verify these hypotheses, statistics are determined

$$F = \frac{R^2}{1-R^2} * \frac{n - \frac{k(k+1)}{2} - 1}{\frac{k(k+1)}{2}} \quad (31)$$

which have a Fisher-Snedecor distribution with  $(k(k+1)/2, n - k(k+1)/2)$  degrees of freedom. For the significance level  $\alpha$ , the critical value  $F^*$  is determined. If  $F \leq F^*$  there is no reason to reject the null hypothesis  $H_0$  (the multiple correlation coefficient  $R$  is insignificantly different from 0), so the fit of the model to the data is too weak. On the other hand, if  $F > F^*$ , the hypothesis  $H_0$  should be rejected in favour of the alternative hypothesis  $H_1$  (the multiple correlation coefficient  $R$  is significantly different from 0), then the fit of the model to the data is sufficiently high.

### Study of the significance of structural parameters

In order to improve the quality of prediction of the model (3), the significance of structural parameters is tested, and therefore the question of whether the transformed variables, squares of these variables and interactions significantly affect the value of the dependent variable can be answered. First, the covariance matrix of structural parameters is estimated

$$D(\beta) = \frac{\sum_{i=1}^n \varepsilon_i^2}{n - \frac{k(k+1)}{2} - 1} (\Pi^T \Pi)^{-1} \quad (32)$$

where the variance of the model parameter is located on the diagonal. The standard deviation of the model parameter is determined as follows:

$$S(\beta_i) = \sqrt{D_i(\beta)} \quad (33)$$

for  $i \in \{0; 1; \dots; k; 11; \dots; 1k; 12; \dots; k-1, k\}$ .

For each parameter  $\beta_i, i \in \{0; 1; \dots; k; 11; \dots; kk; 12; \dots; k-1, k\}$  at the significance level  $\alpha$ , the working hypothesis is verified

$$H_0: \beta_i = 0$$

against the alternative hypothesis

$$H_1: \beta_i \neq 0$$

The statistics

$$I_i = \frac{|\hat{\beta}_i|}{s(\beta_i)} \quad (34)$$

have a t-distribution for  $n - k(k + 1)/2 - 1$  degrees of freedom. If  $I_i \leq I^*$ , there is no reason to reject the null hypothesis  $H_0$ , and the structural parameter  $\beta_i$  is insignificantly different from 0. However,  $I_i > I^*$ , we reject the null hypothesis  $H_0$  in favour of the alternative hypothesis  $H_1$  (the structural parameter  $\beta_i$  is significantly different from 0). To improve the forecasting of the endogenous variable, predictors corresponding to the structural parameters in model (3), which are insignificantly different from 0, are removed.

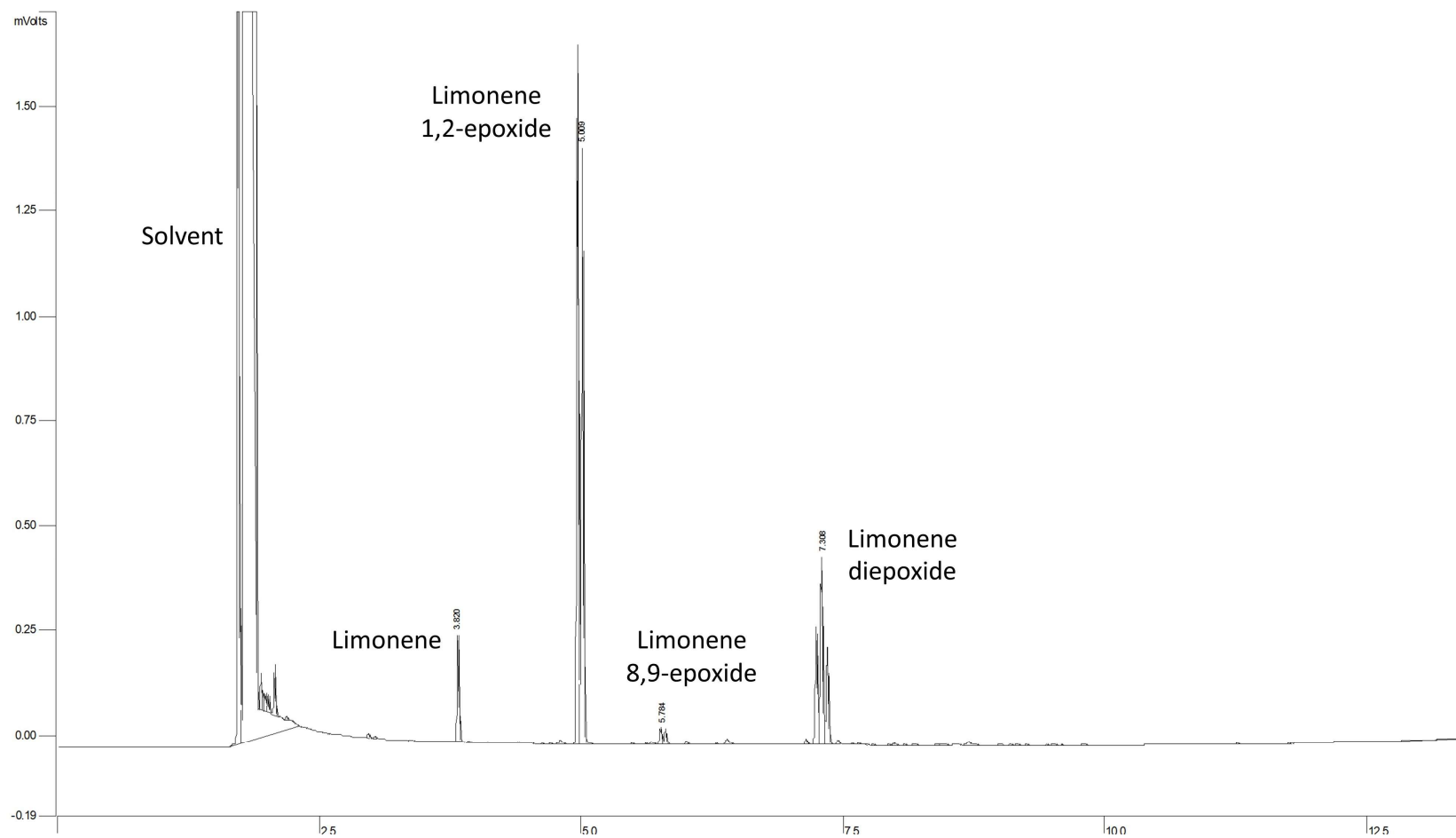


Figure S1. GC-FID chromatogram of a reaction mixture of (*R*)-(+)-limonene epoxidation by *Cladosporium cladosporioides* 01

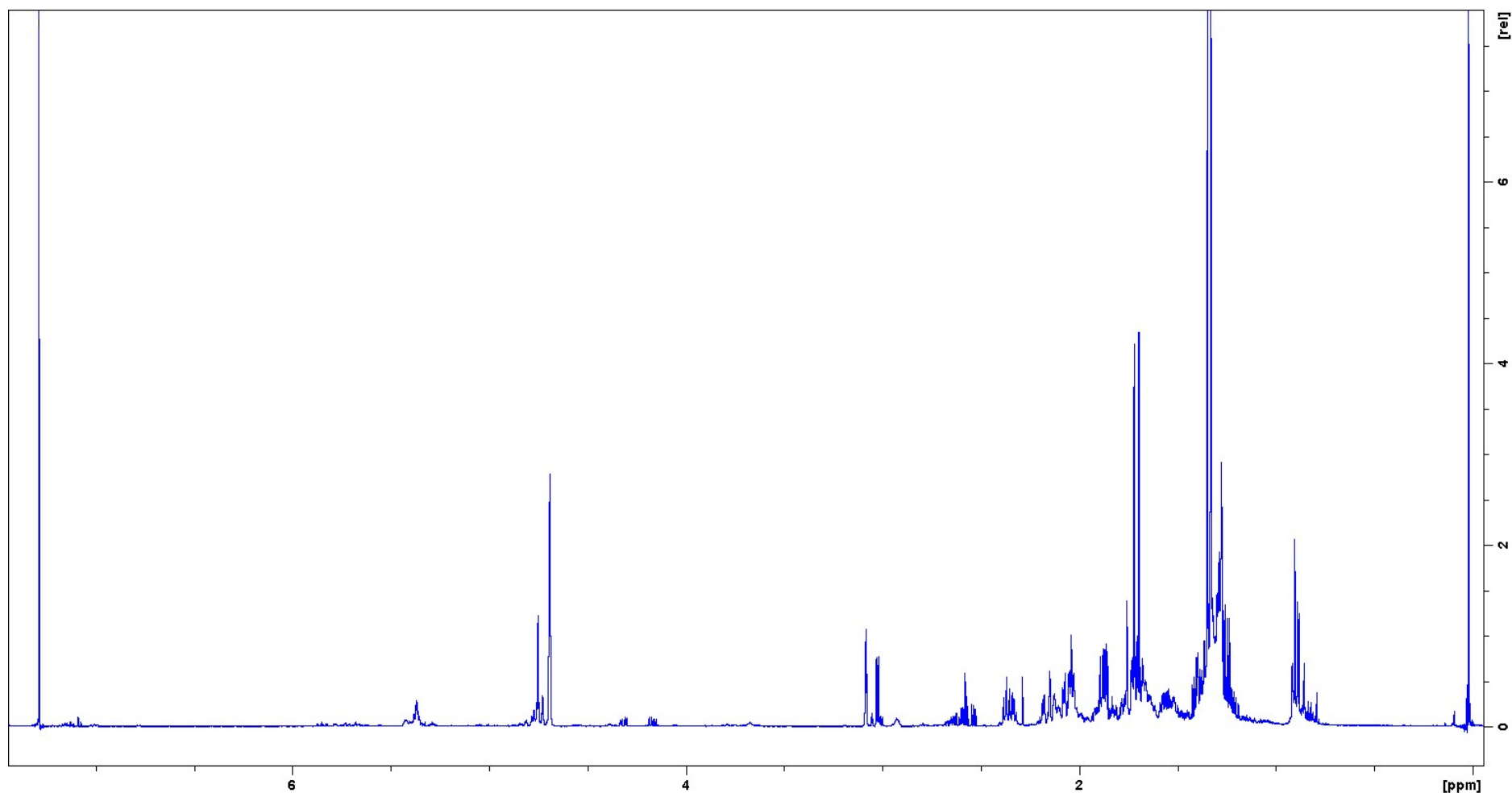


Figure S2. <sup>1</sup>H NMR spectra of a reaction mixture of (*R*)-(+)-limonene oxidation by *Cladosporium cladosporioides* 01

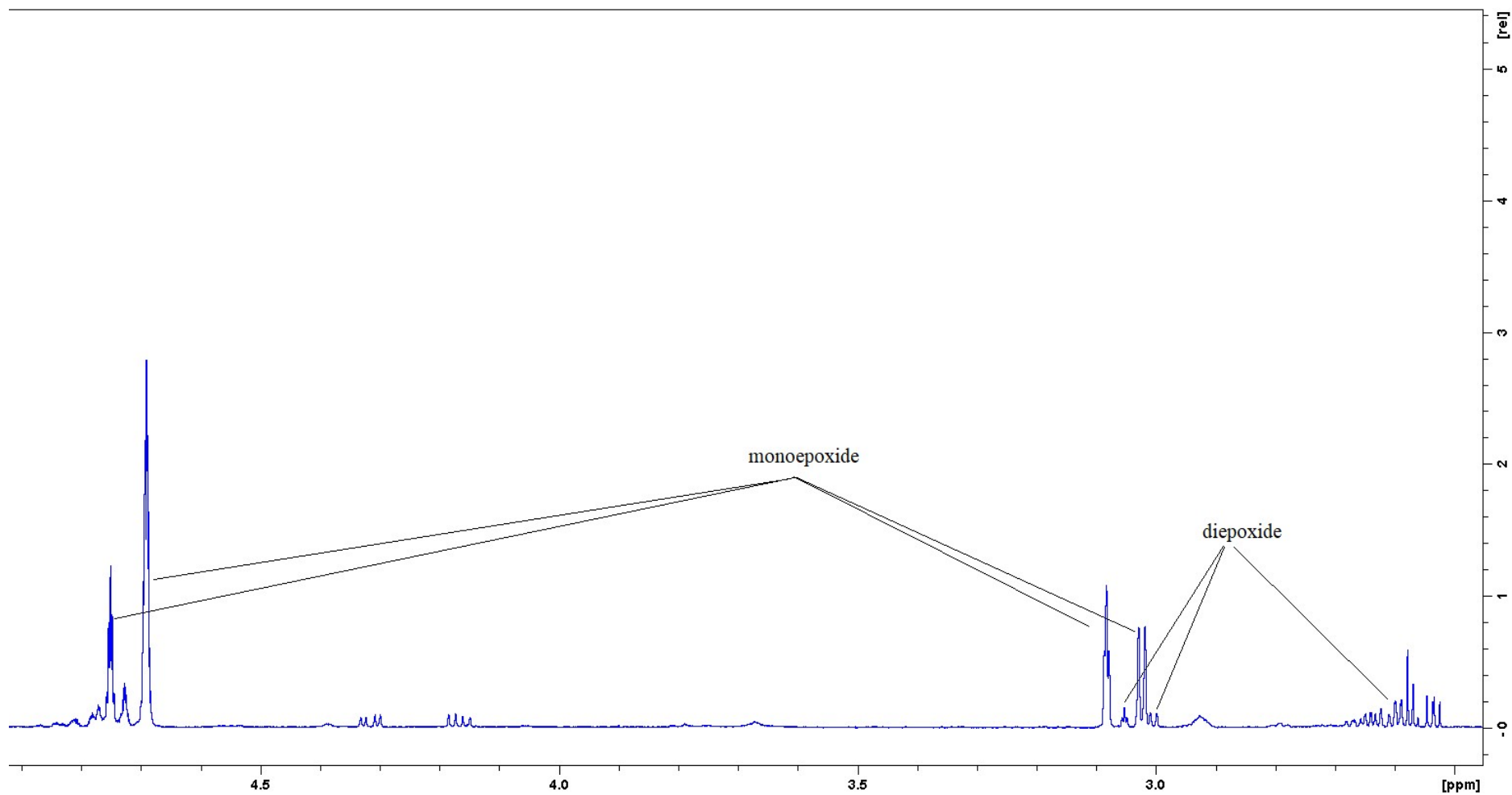


Figure S3. <sup>1</sup>H NMR spectra of a reaction mixture of (*R*)-(+)-limonene oxidation by *Cladosporium cladosporioides* 01 – a spectral region with the most characteristic signals of mono and diepoxide

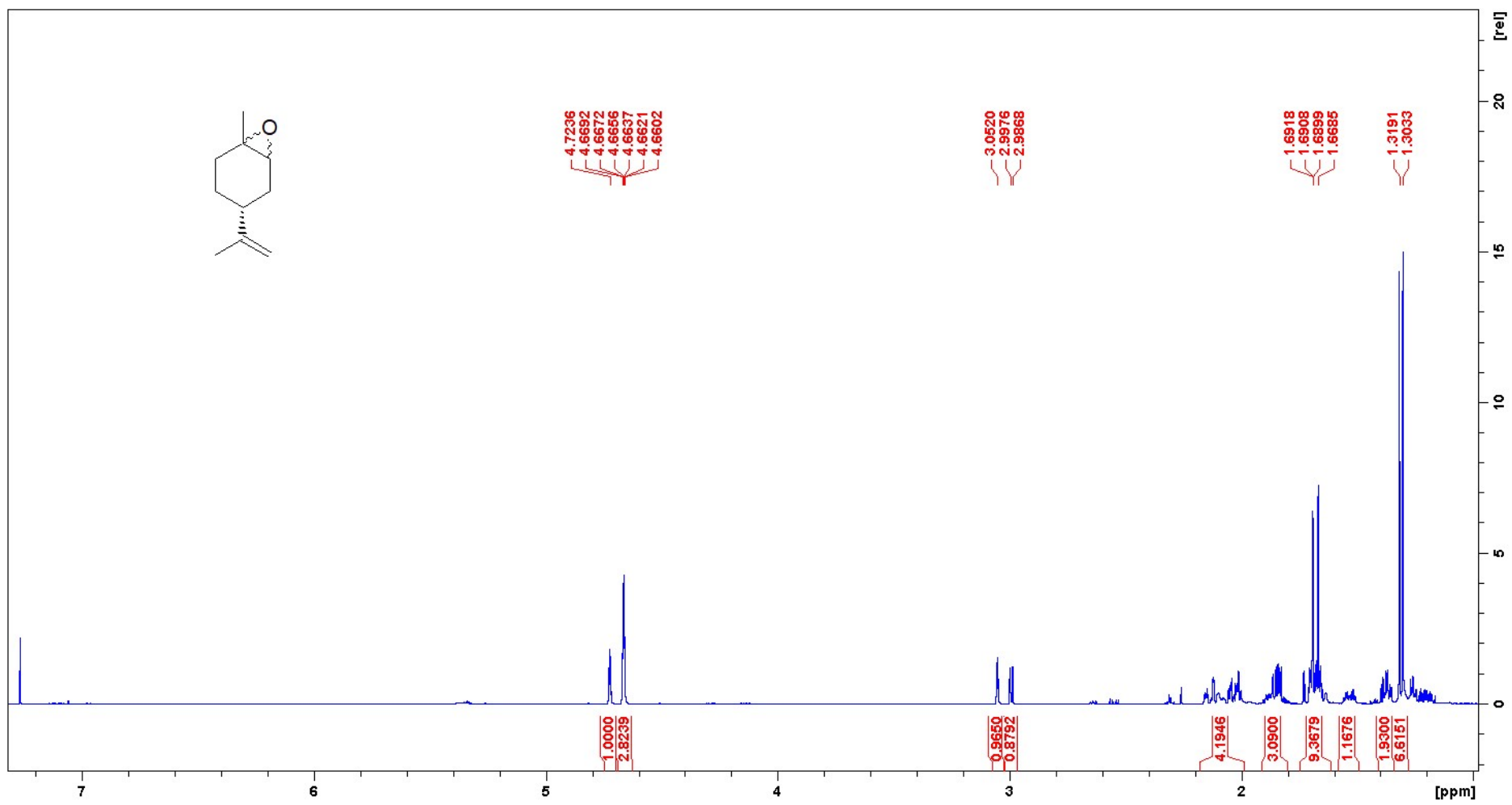


Figure S4. <sup>1</sup>H NMR spectra of limonene epoxide isolated from the reaction mixture of (*R*)-(+)-limonene oxidation by *C. cladosporioides* 01

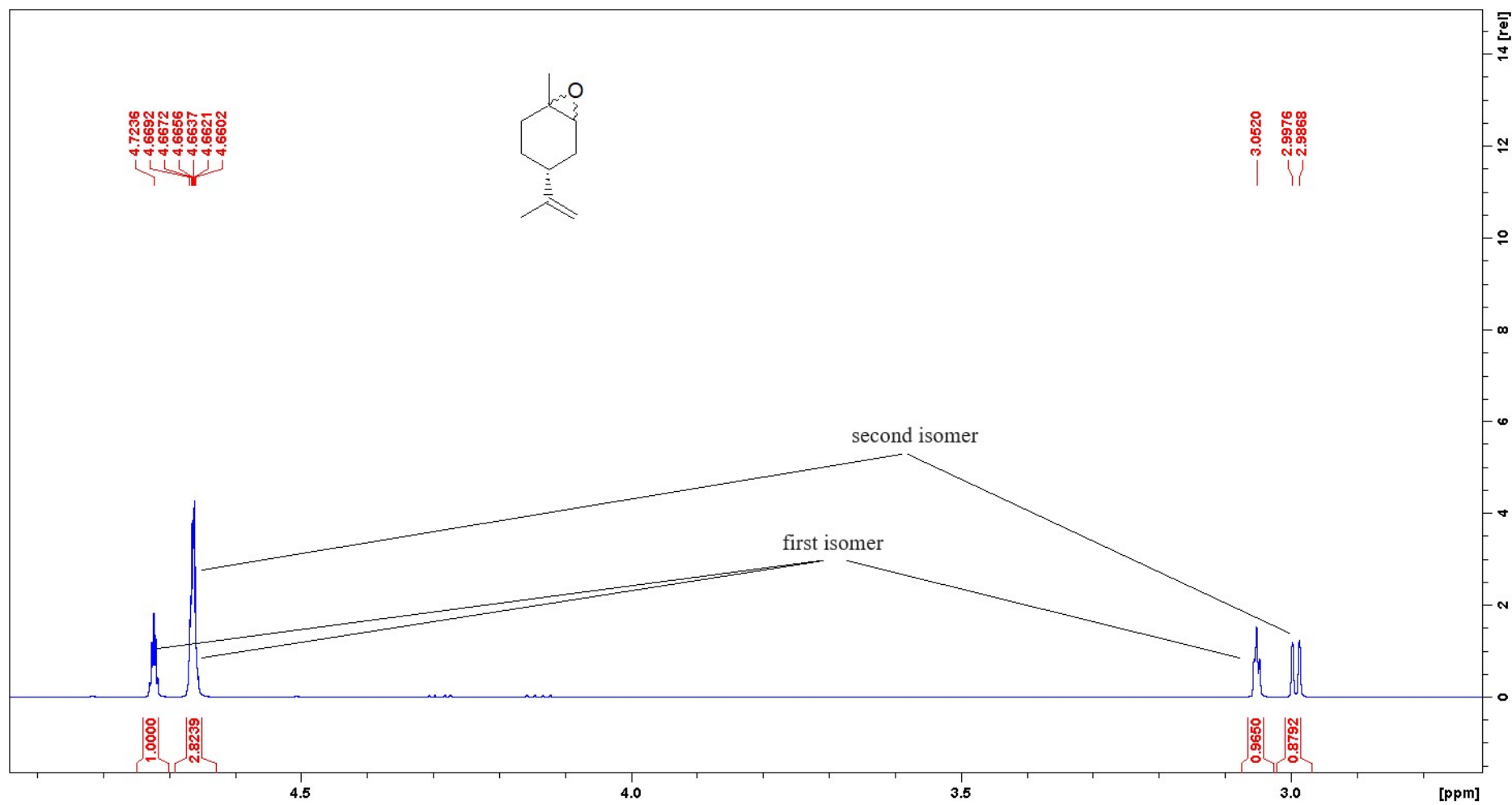


Figure S5. <sup>1</sup>H NMR spectra of limonene epoxide isolated from the reaction mixture of (*R*)-(+)-limonene oxidation by *C. cladosporioides* 01 – the most characteristic signals of limonene monoepoxide



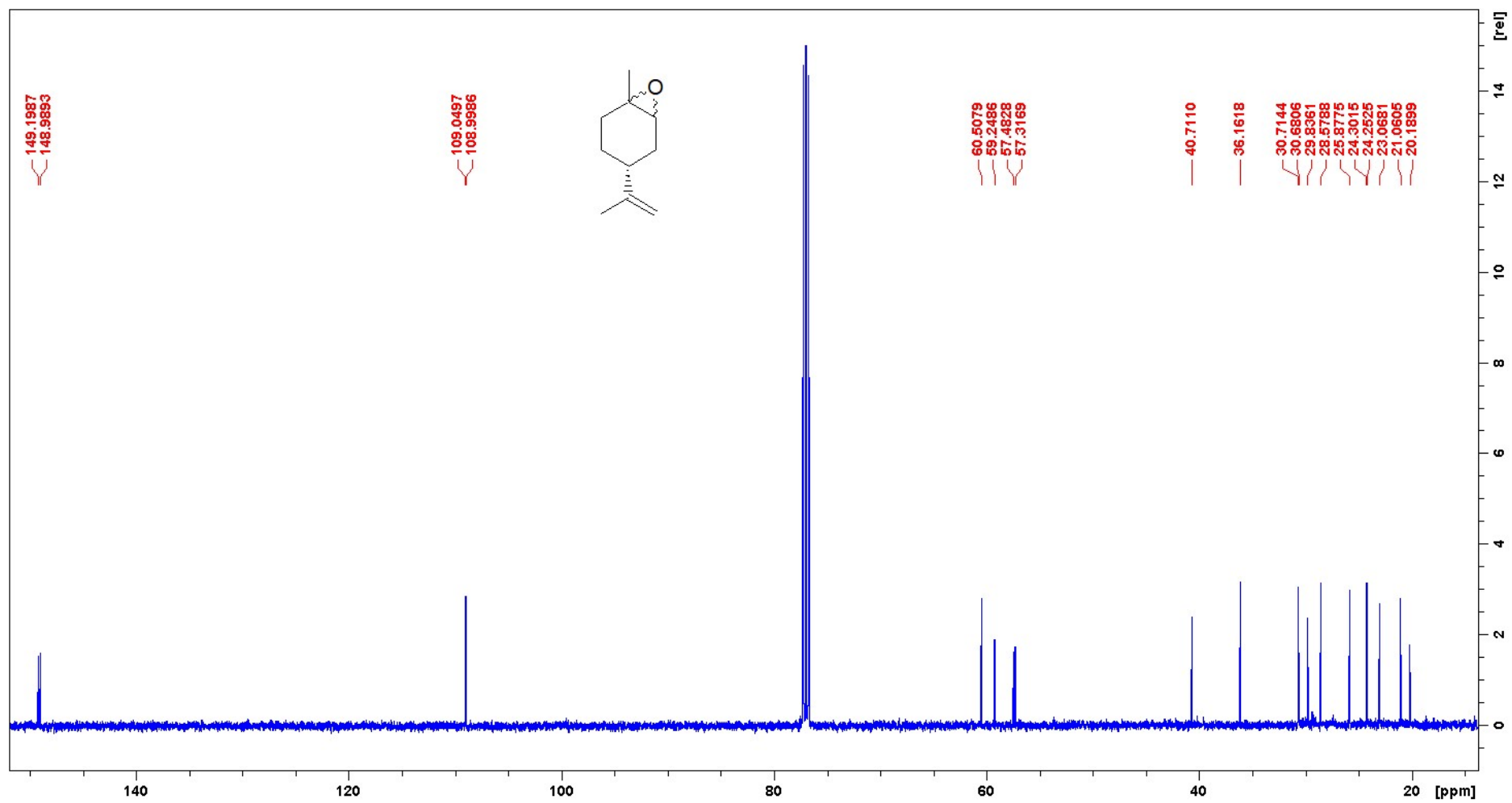


Figure S6.  $^{13}\text{C}$  NMR spectra of limonene epoxide isolated from the reaction mixture of (*R*)-(+)-limonene oxidation by *C. cladosporioides* 01

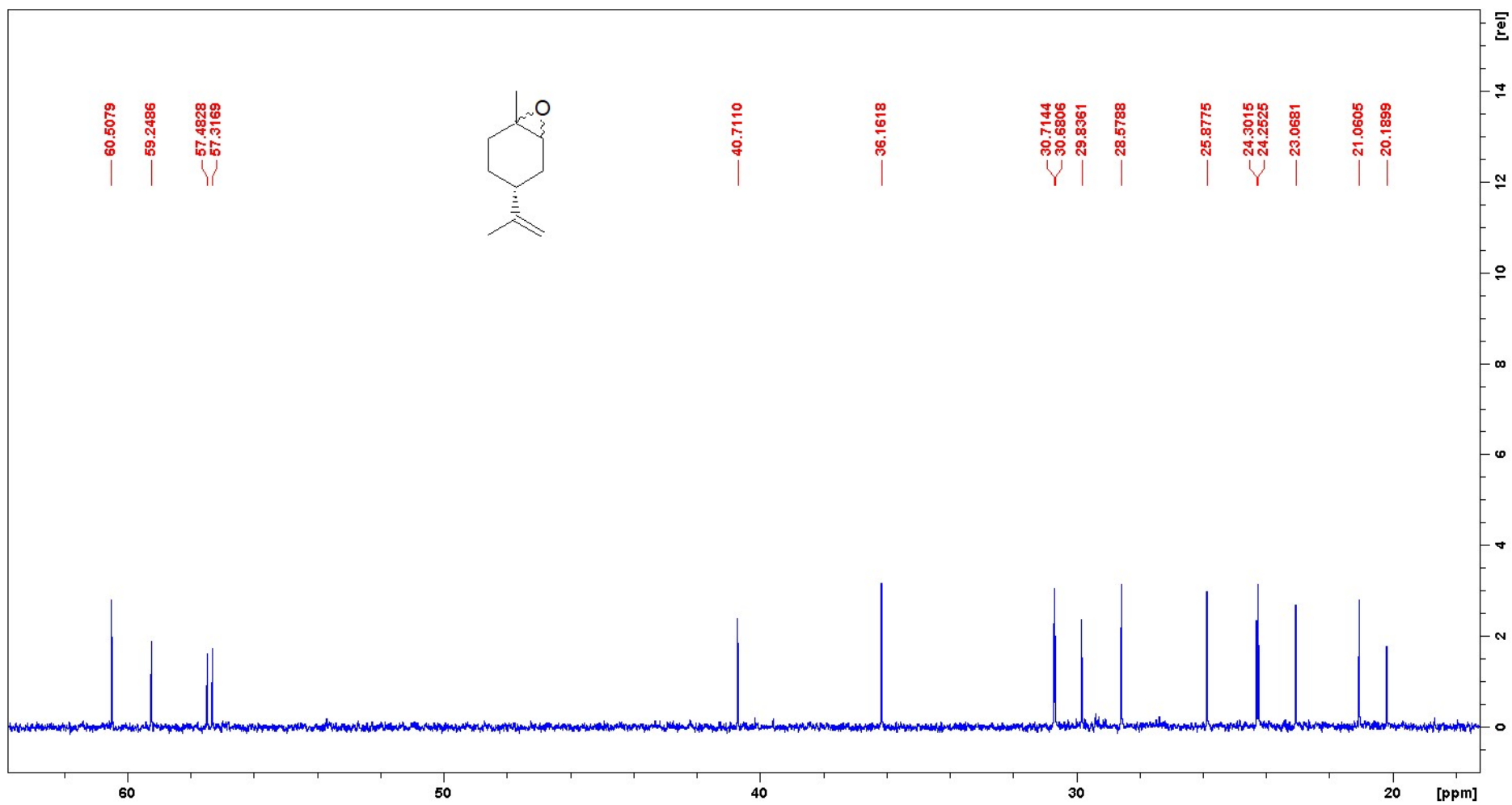


Figure S7.  $^{13}\text{C}$  NMR spectra of limonene epoxide isolated from the reaction mixture of (*R*)-(+)-limonene oxidation by *C. cladosporioides* 01 – aliphatic region

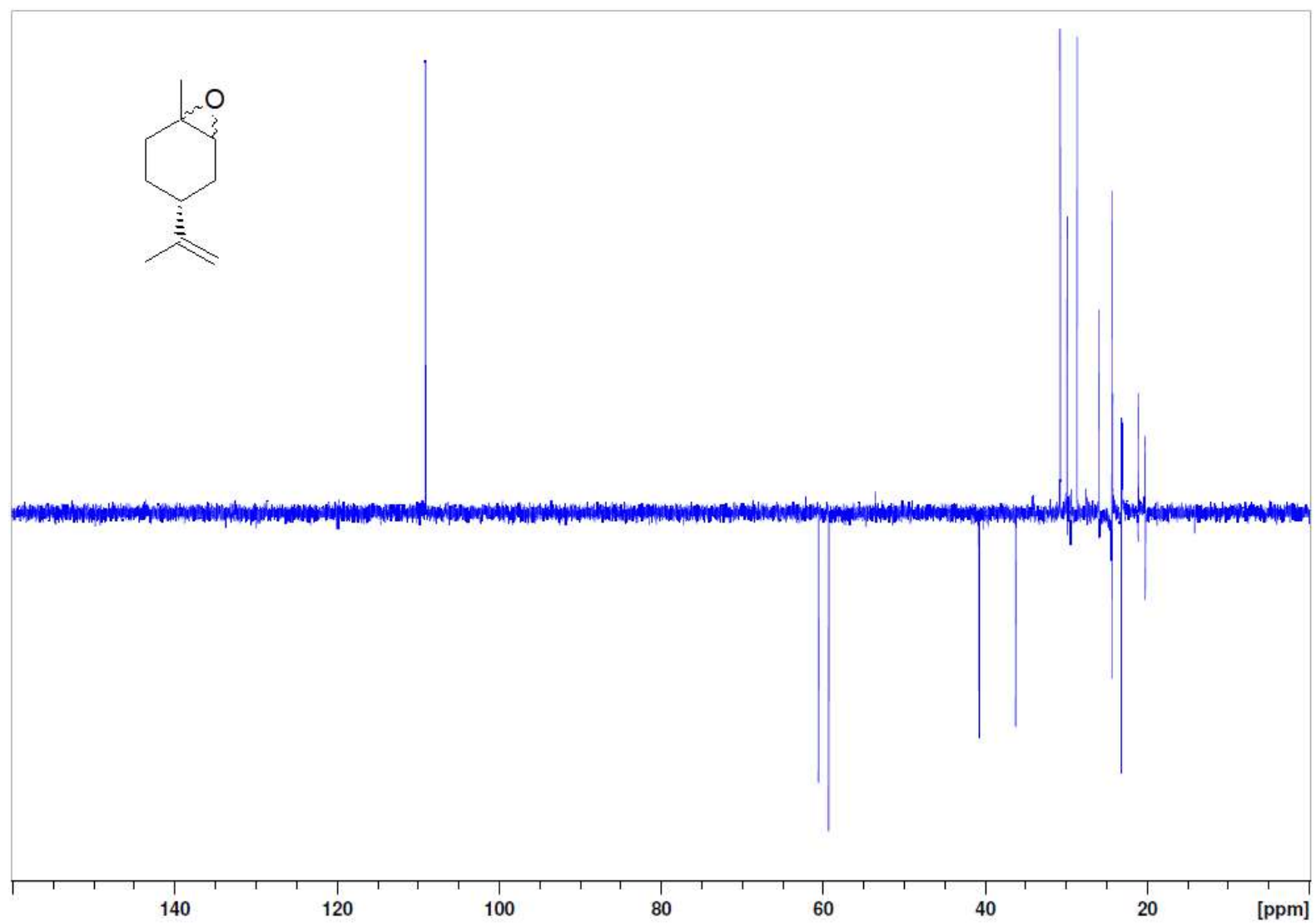


Figure S8. DEPT 135 of limonene epoxide isolated from the reaction mixture of (*R*)-(+)-limonene oxidation by *C. cladosporioides* 01

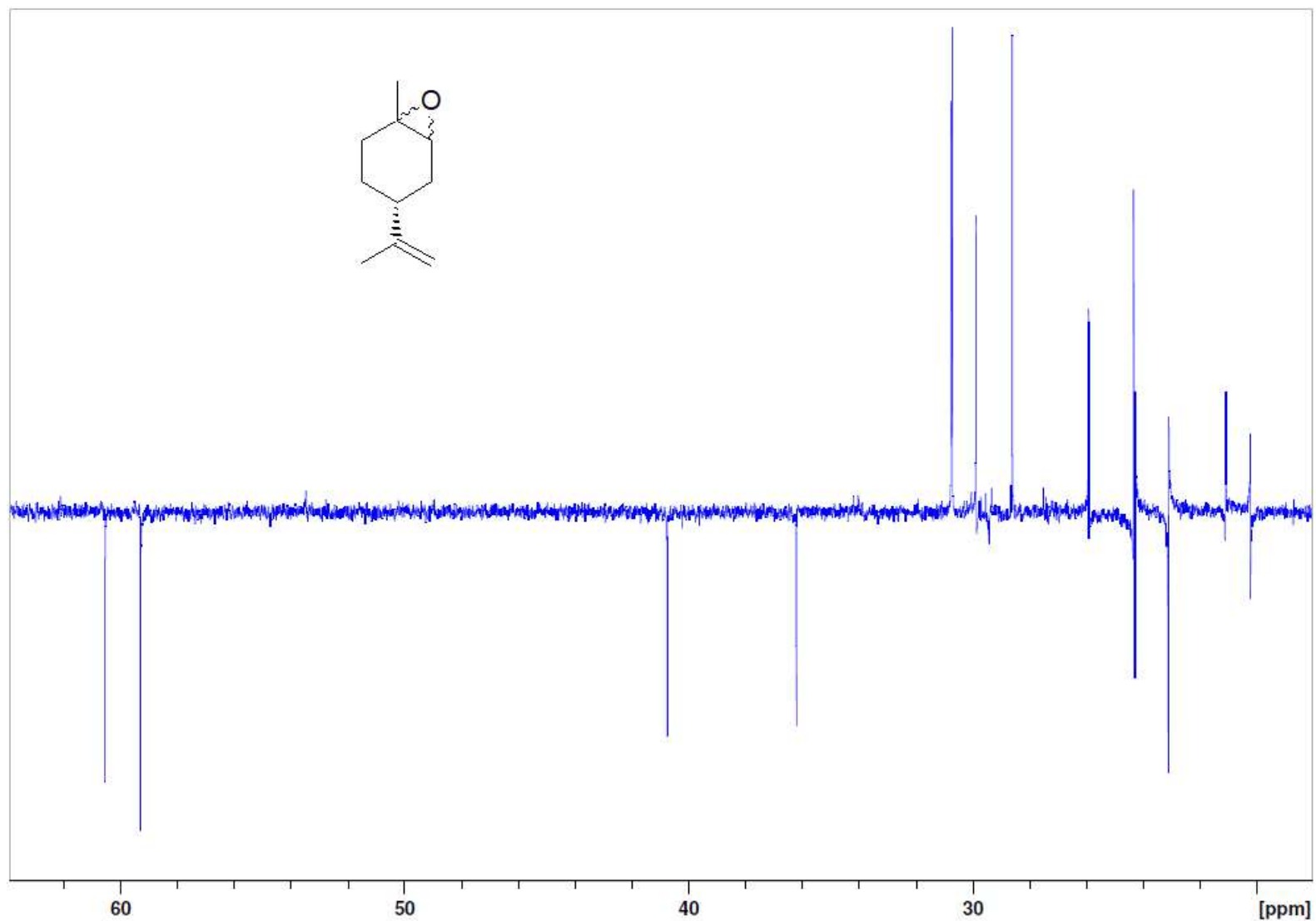


Figure S9. DEPT 135 of limonene epoxide isolated from the reaction mixture of (*R*)-(+)-limonene oxidation by *C. cladosporioides* 01 – aliphatic region

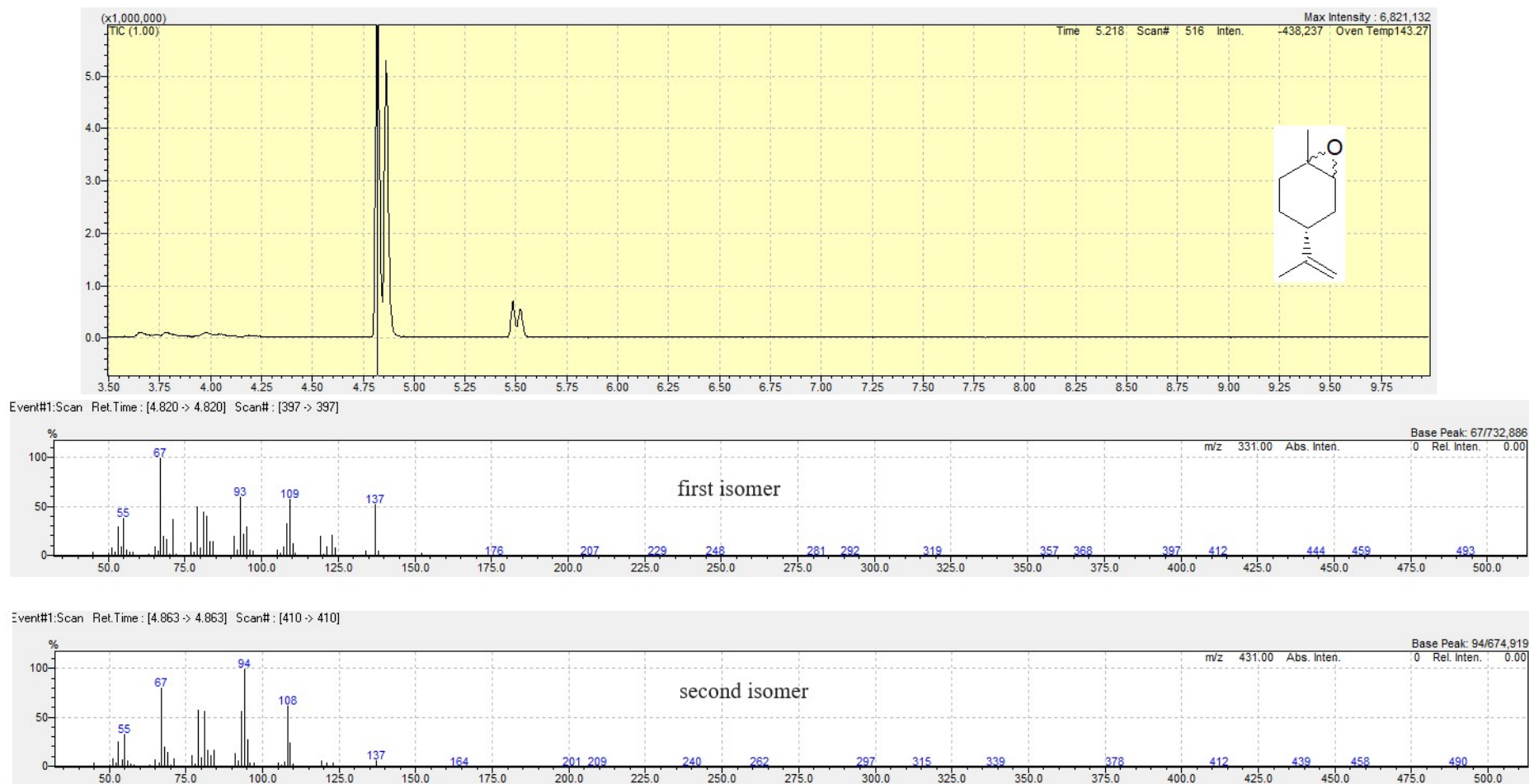


Figure S10. GC-MS analysis of a fraction containing limonene epoxide isolated from the reaction mixture of (*R*)-(+)-limonene oxidation by *Cladosporium cladosporioides* 01

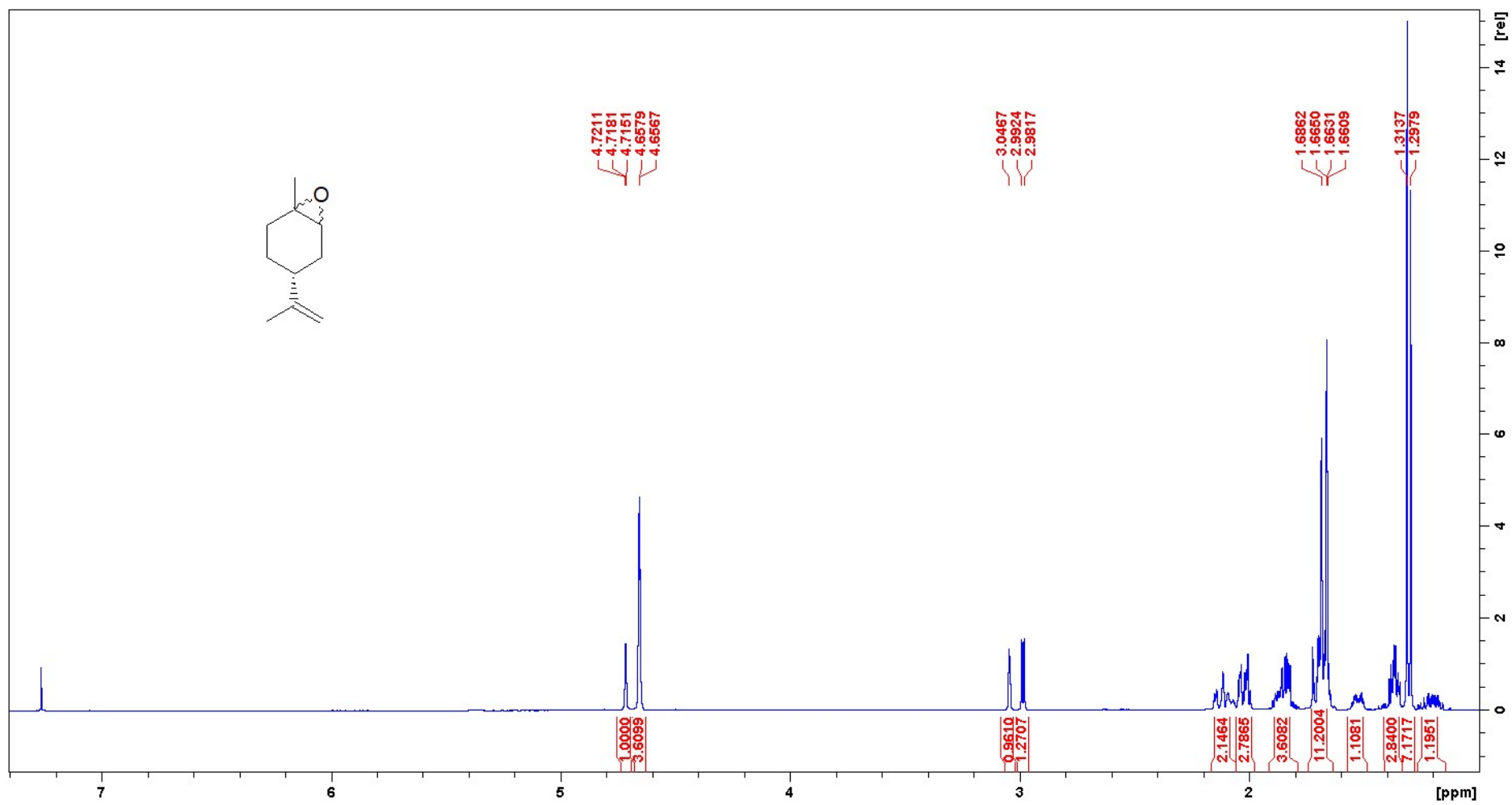


Figure S11. <sup>1</sup>H NMR spectra of commercial (+)-limonene epoxide

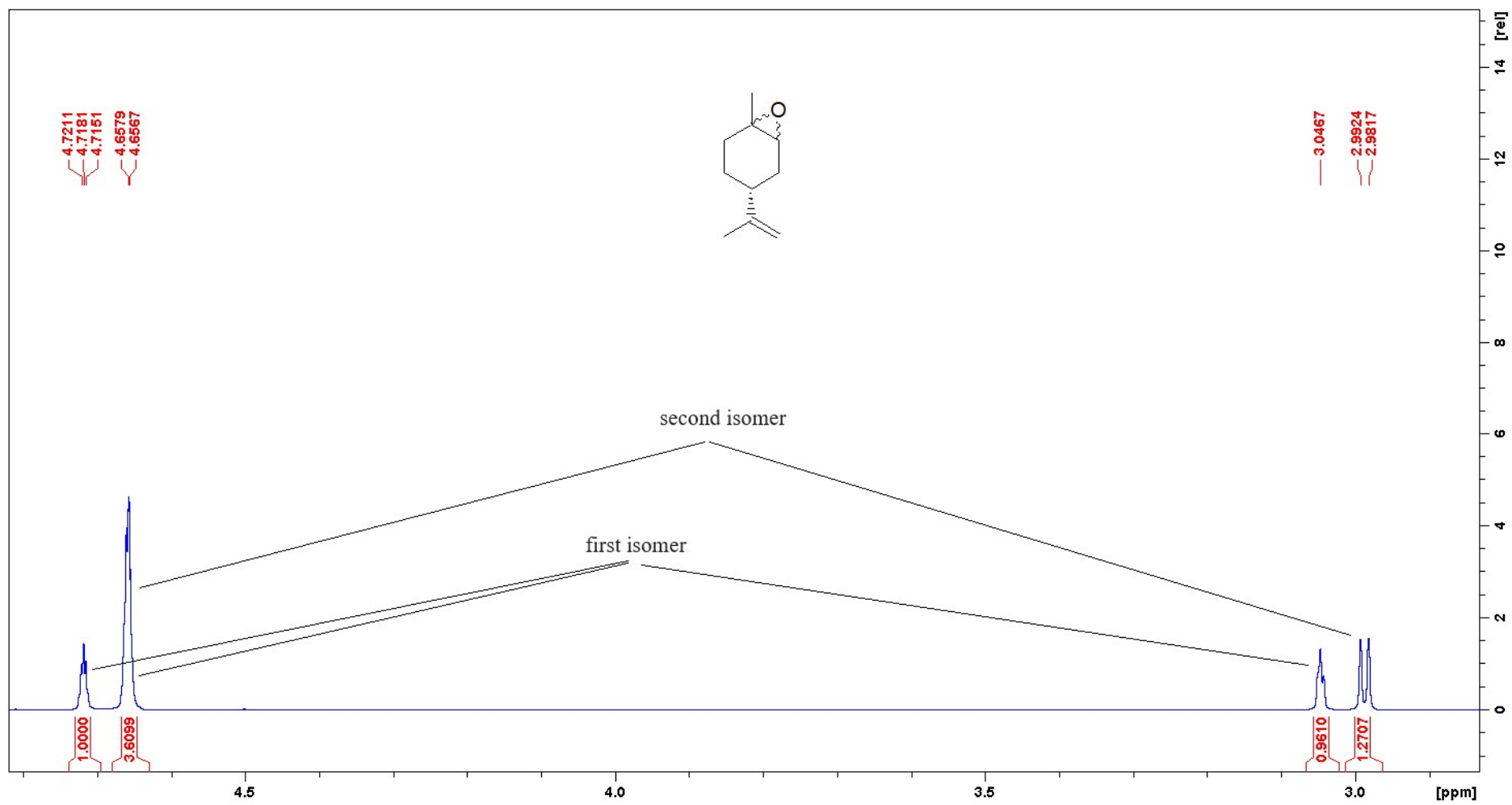


Figure S12.  $^1\text{H}$  NMR spectra of commercial (+)-limonene epoxide – a region with the most characteristic signals of monoepoxide

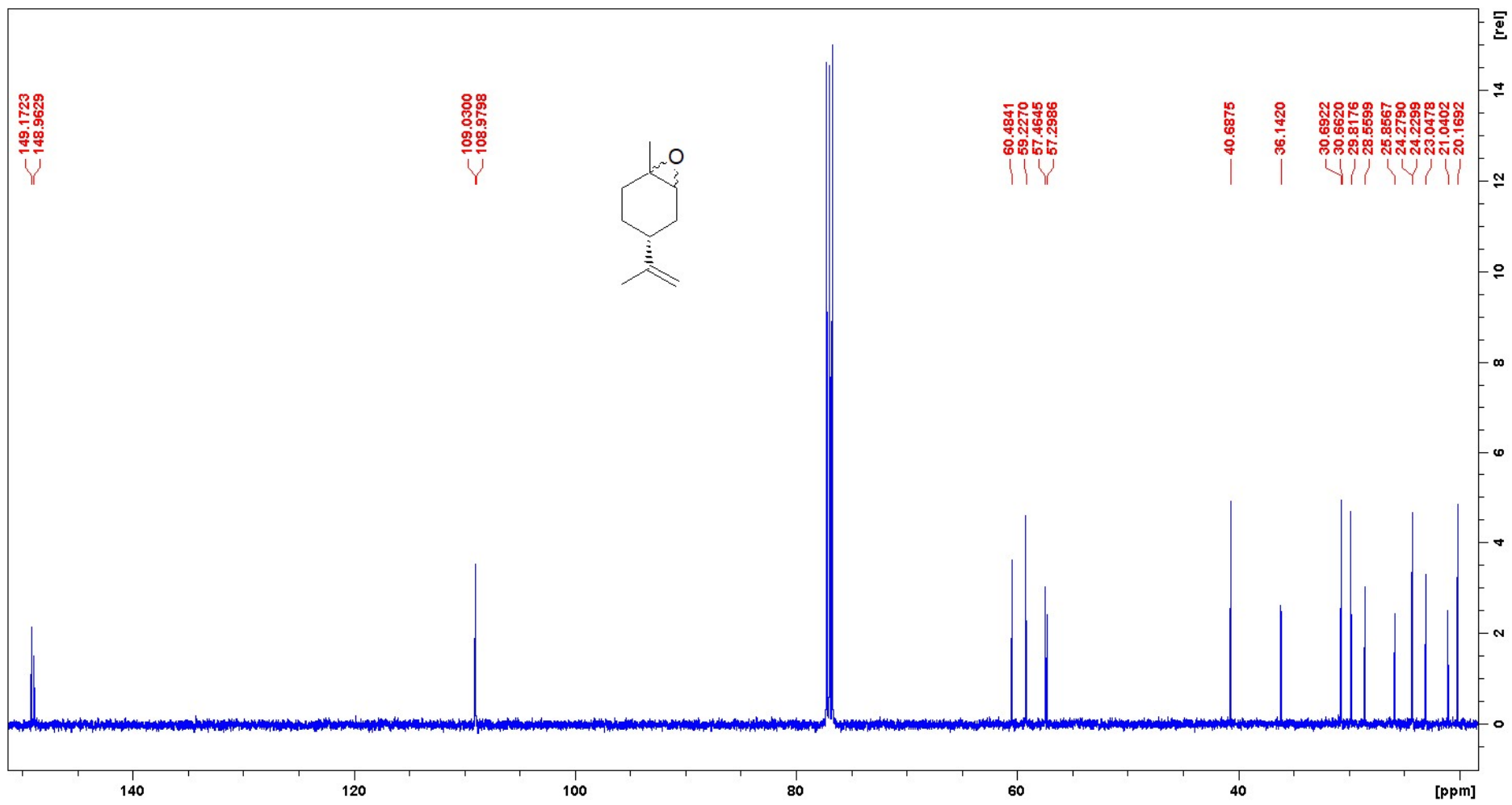


Figure S13.  $^{13}\text{C}$  NMR spectra of commercial (+)-limonene epoxide



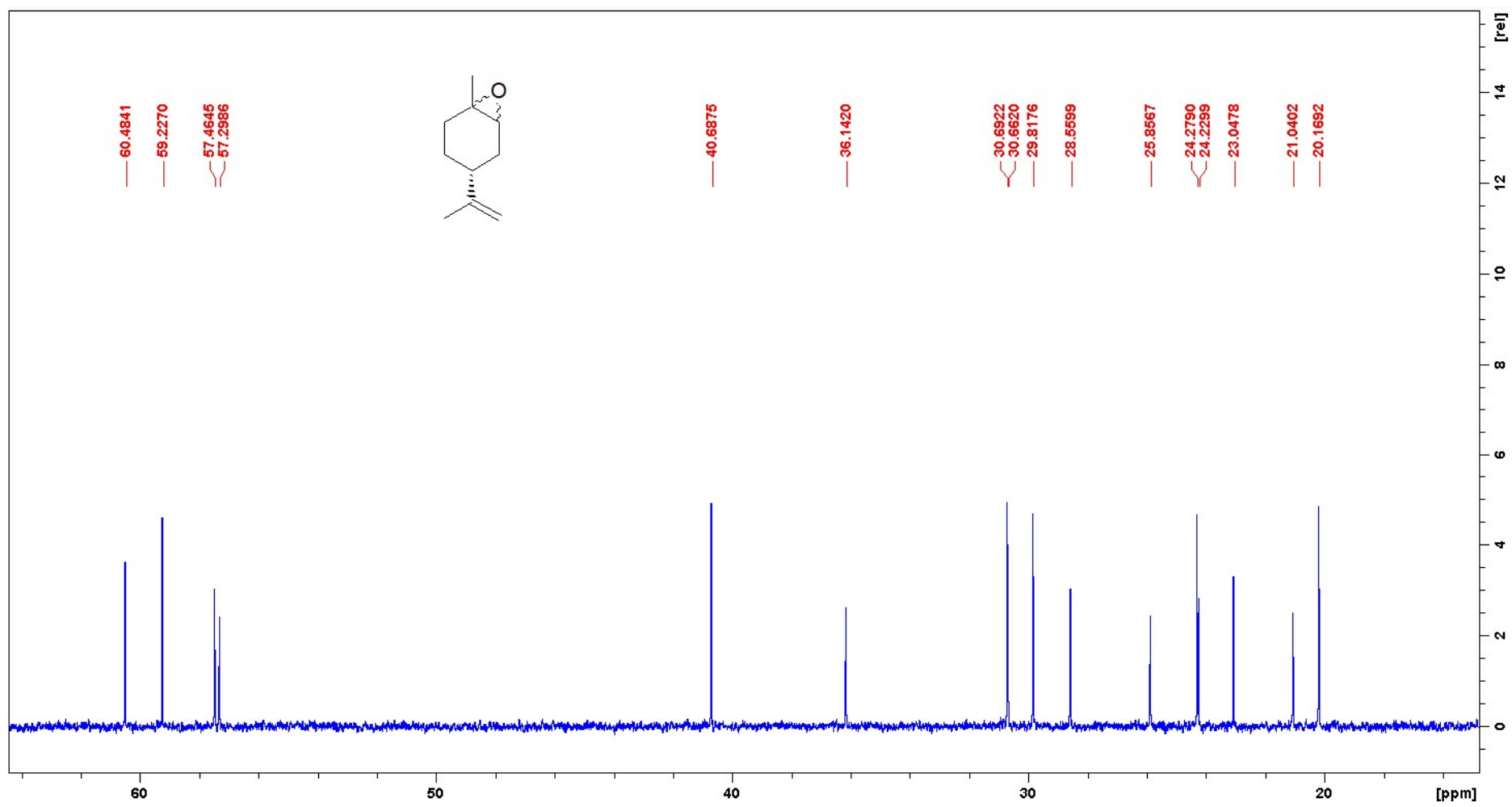


Figure S14. <sup>13</sup>C NMR spectra of commercial (+)-limonene epoxide – aliphatic region

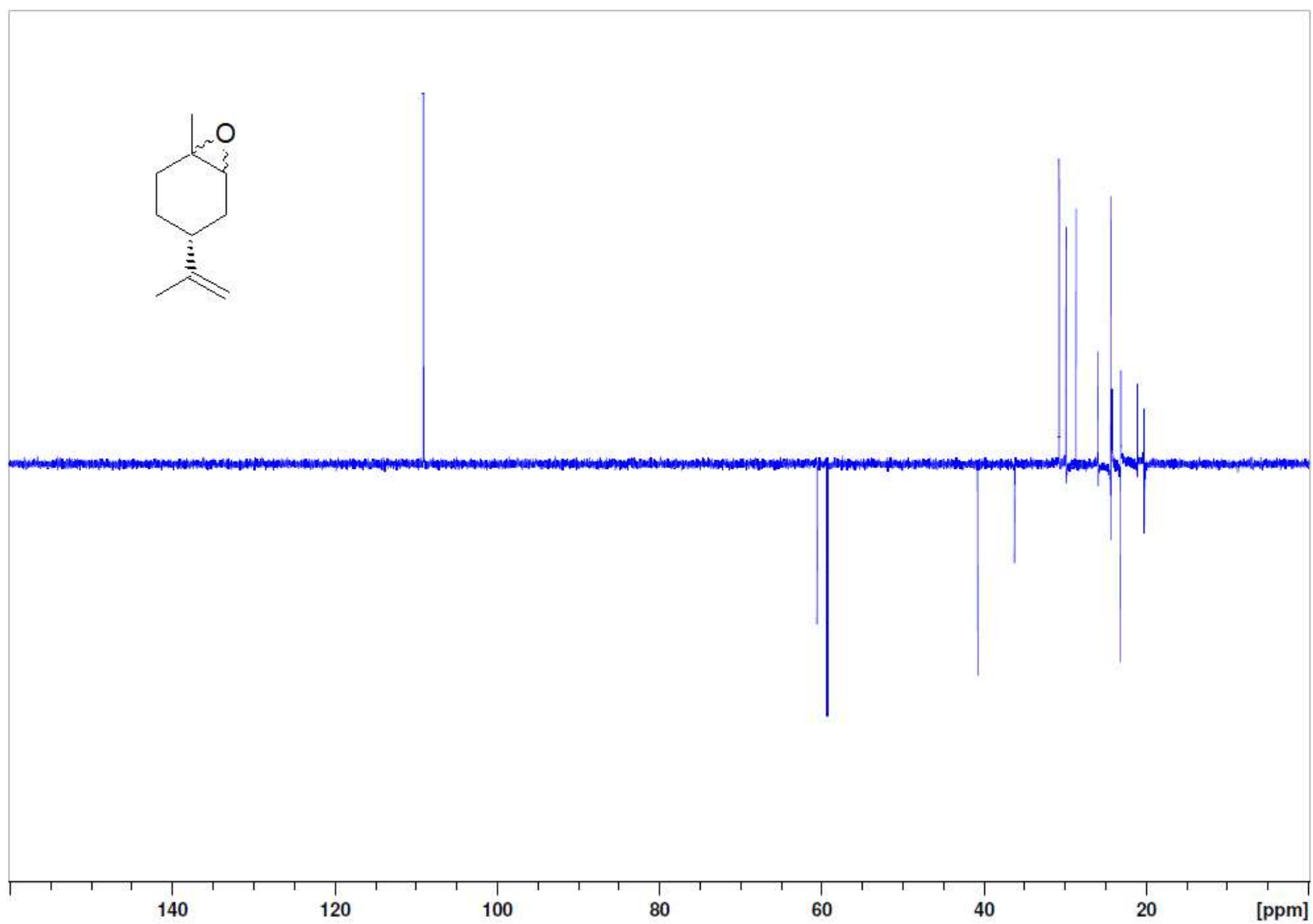


Figure S15. DEPT 135 of commercial (+)-limonene epoxide

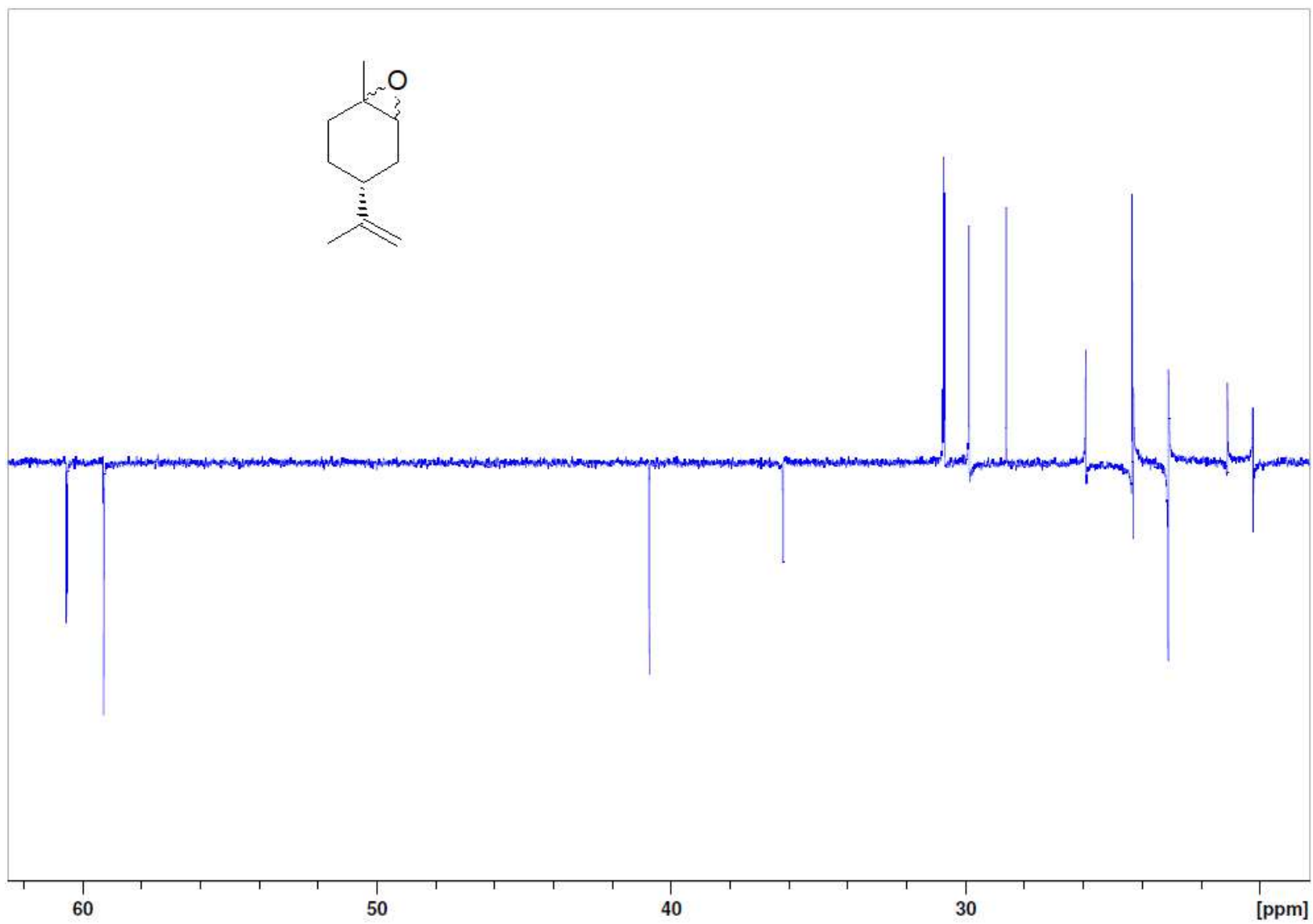


Figure S16. DEPT 135 of commercial (+)-limonene epoxide – aliphatic region

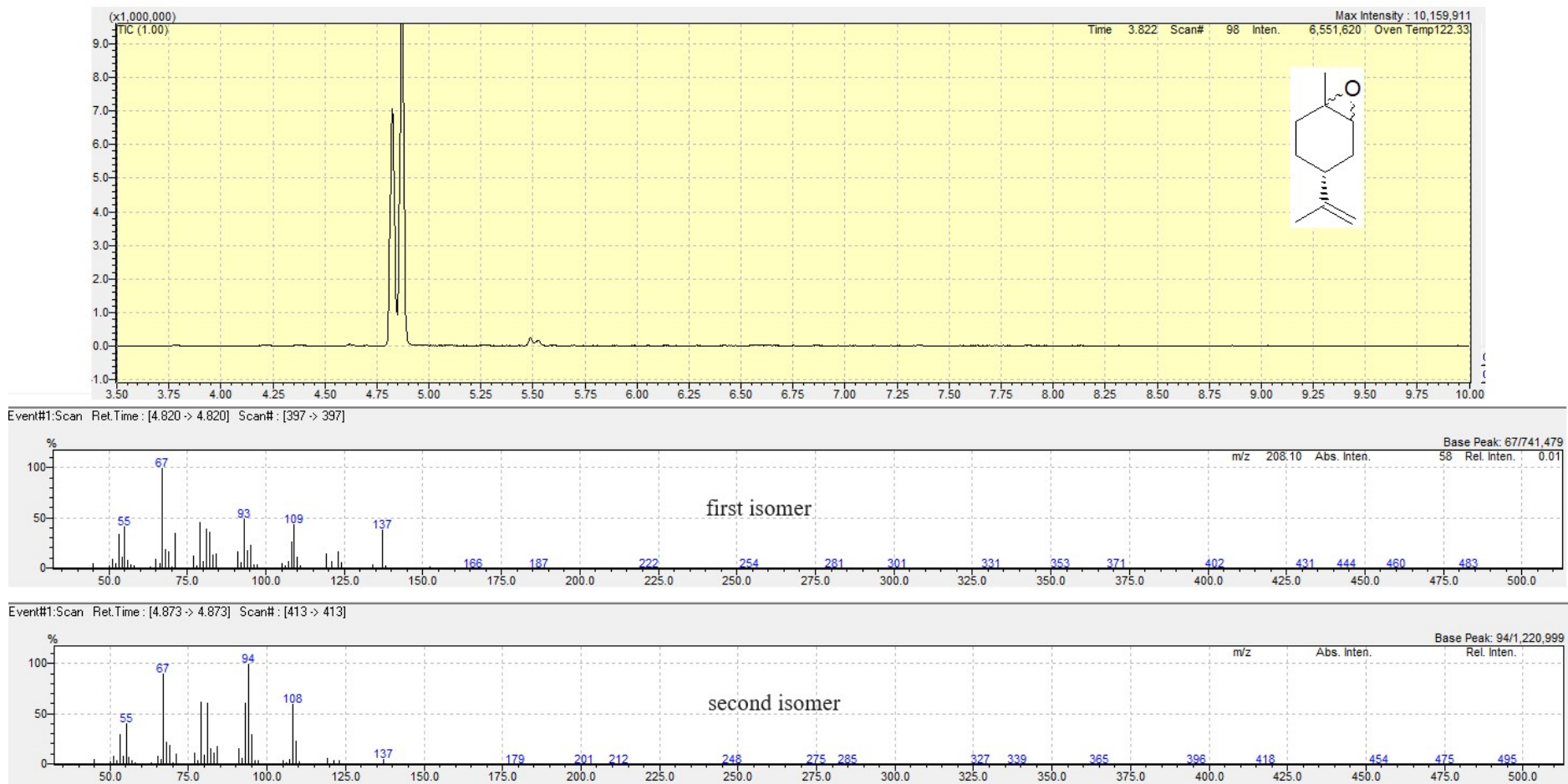


Figure S17. GC-MS of commercial (+)-limonene epoxide

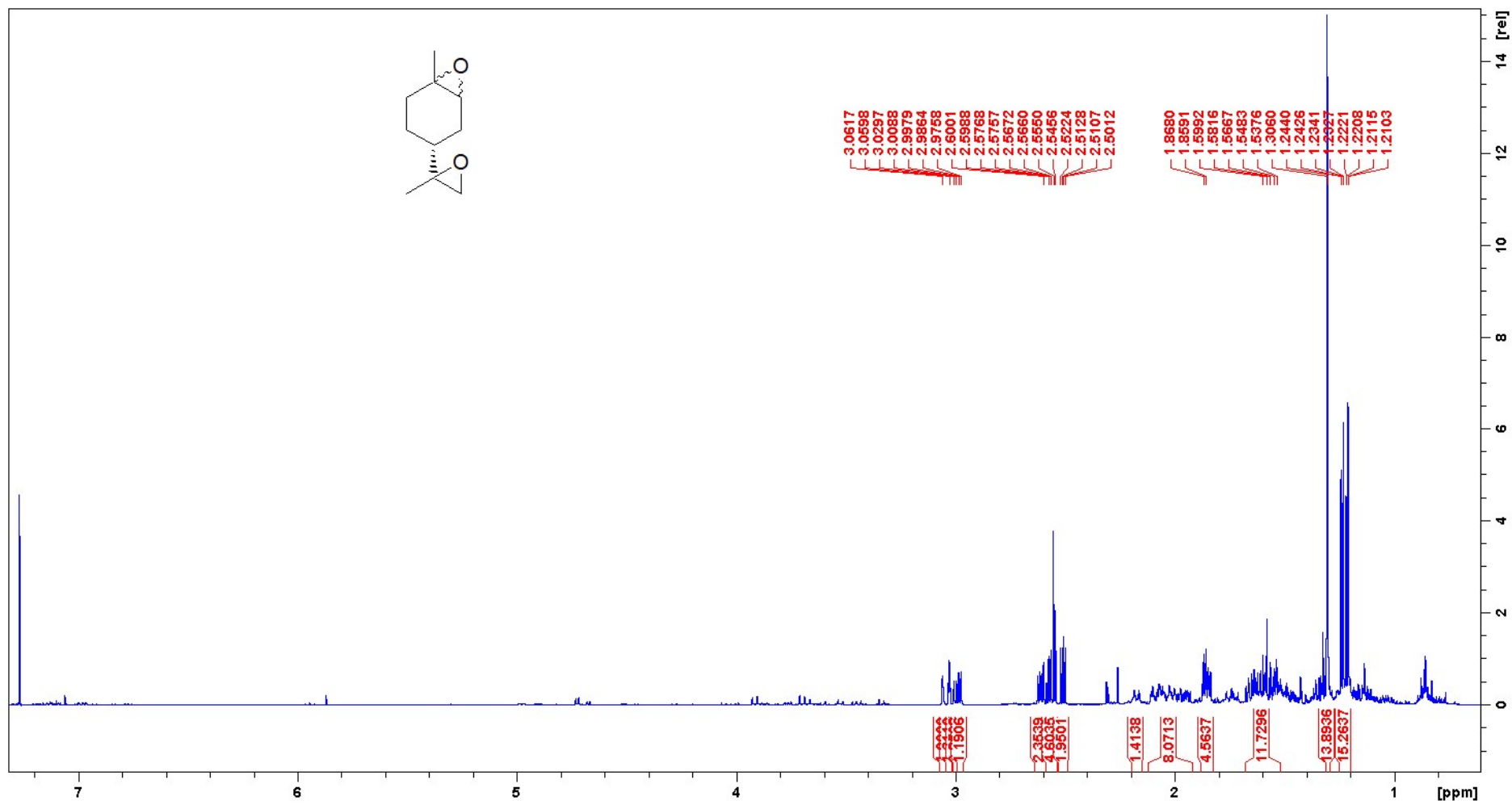


Figure S18. <sup>1</sup>H NMR spectra of crude limonene diepoxide obtained from commercial (+)-limonene epoxide

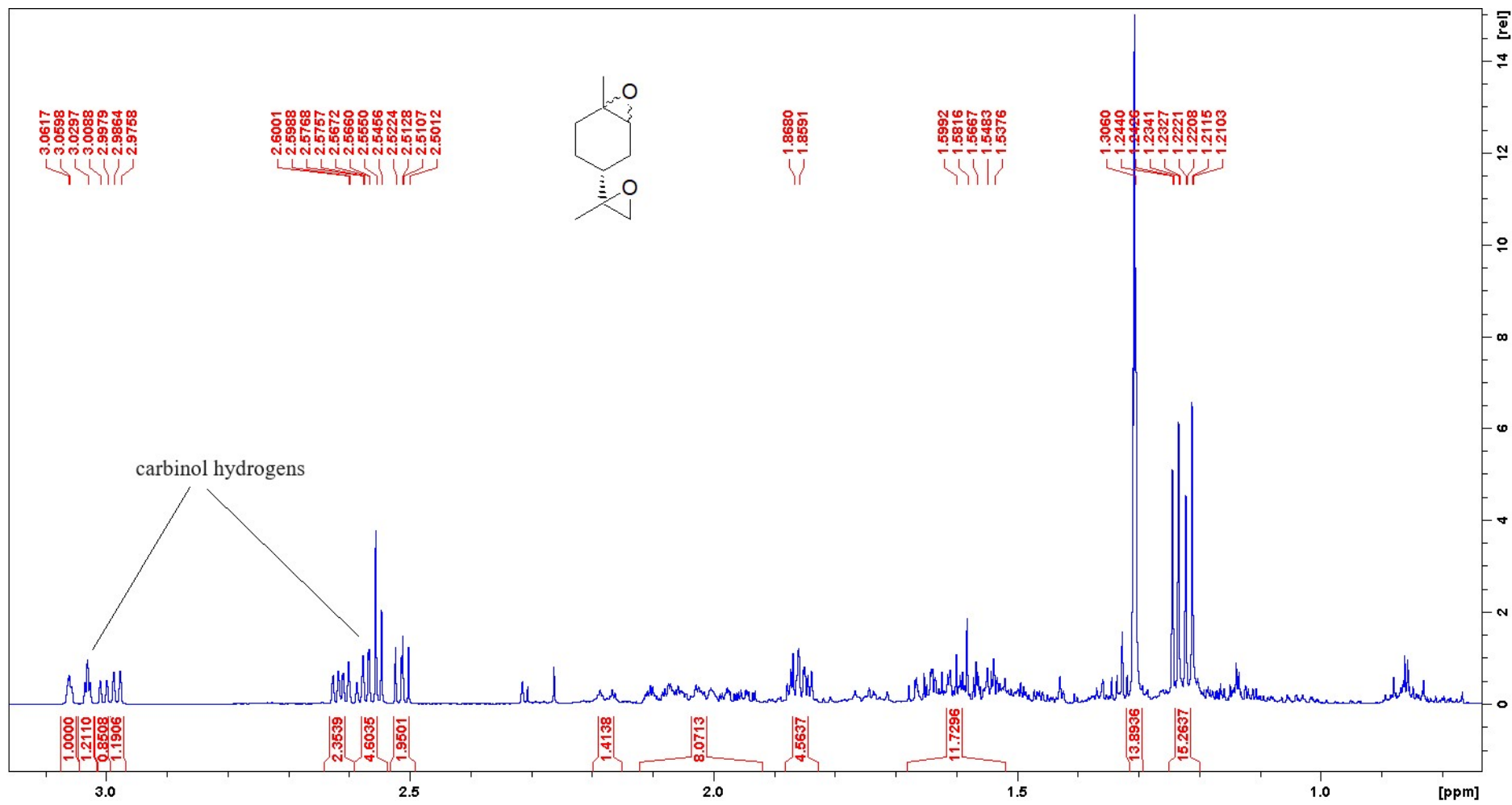


Figure S19.  $^1\text{H}$  NMR spectra of crude limonene diepoxide obtained from commercial (+)-limonene epoxide – aliphatic region

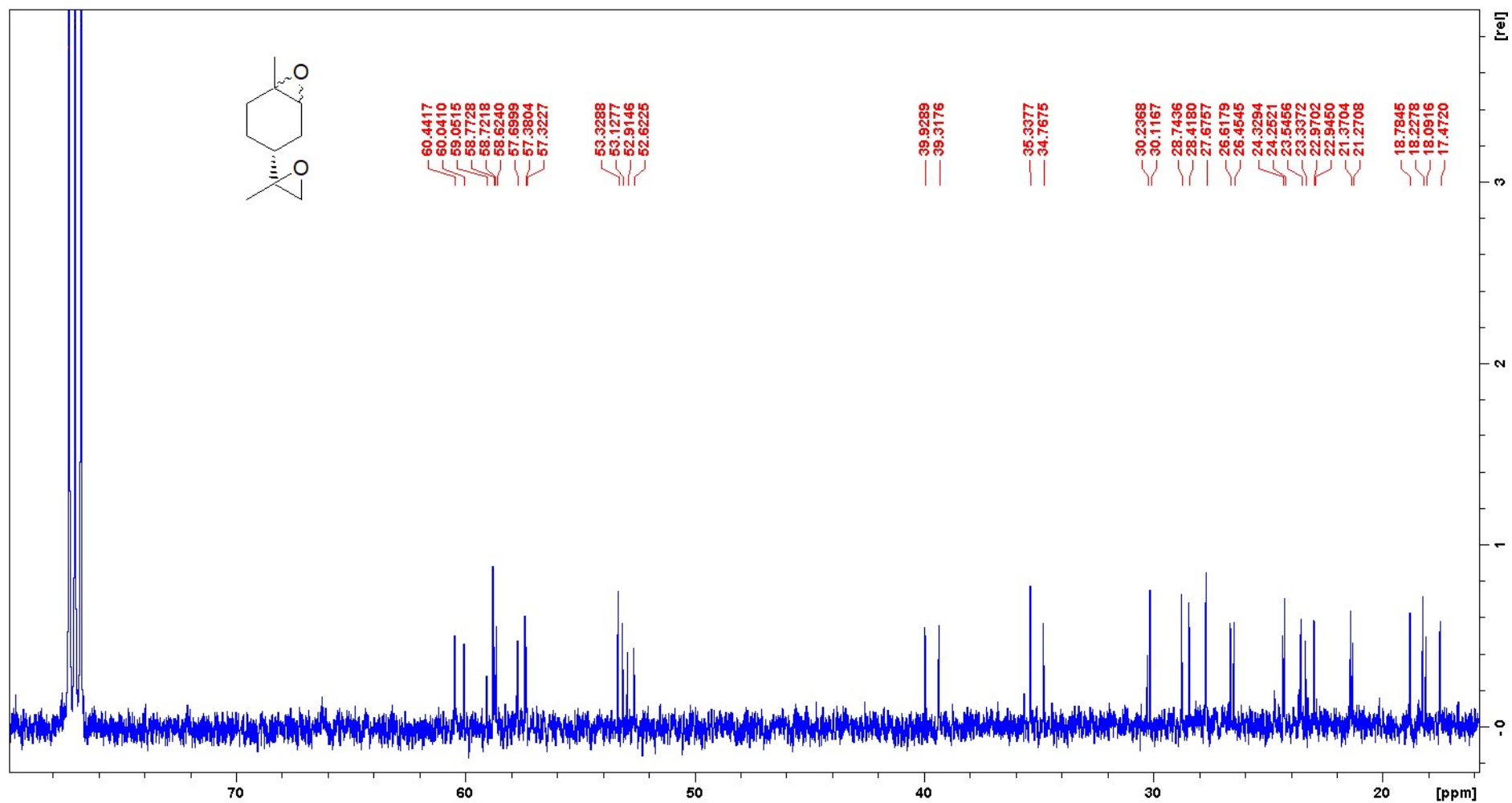


Figure S20.  $^{13}\text{C}$  NMR spectra of crude limonene diepoxide obtained from commercial (+)-limonene epoxide

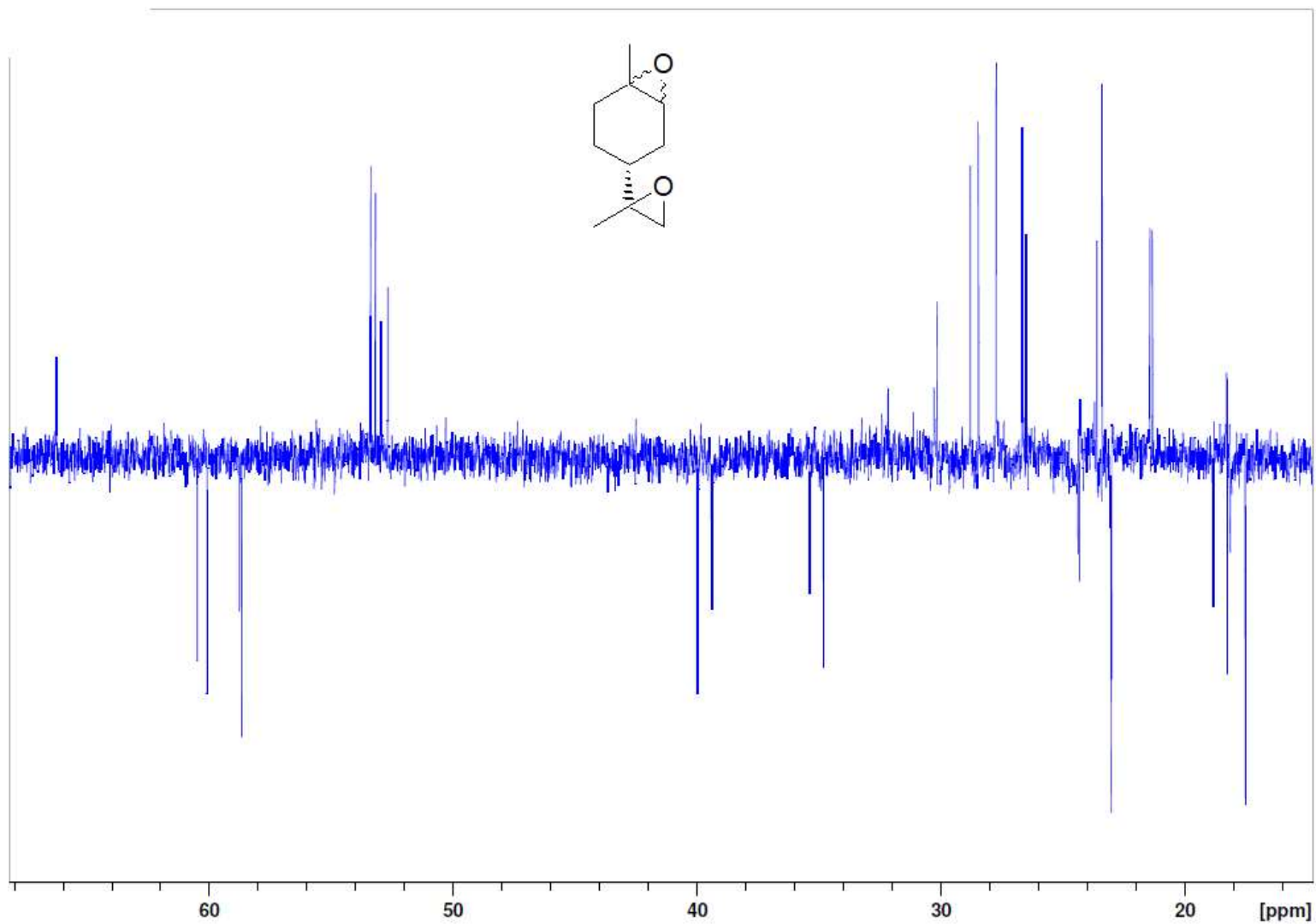


Figure S21. DEPT135 of crude limonene diepoxide obtained from commercial (+)-limonene epoxide



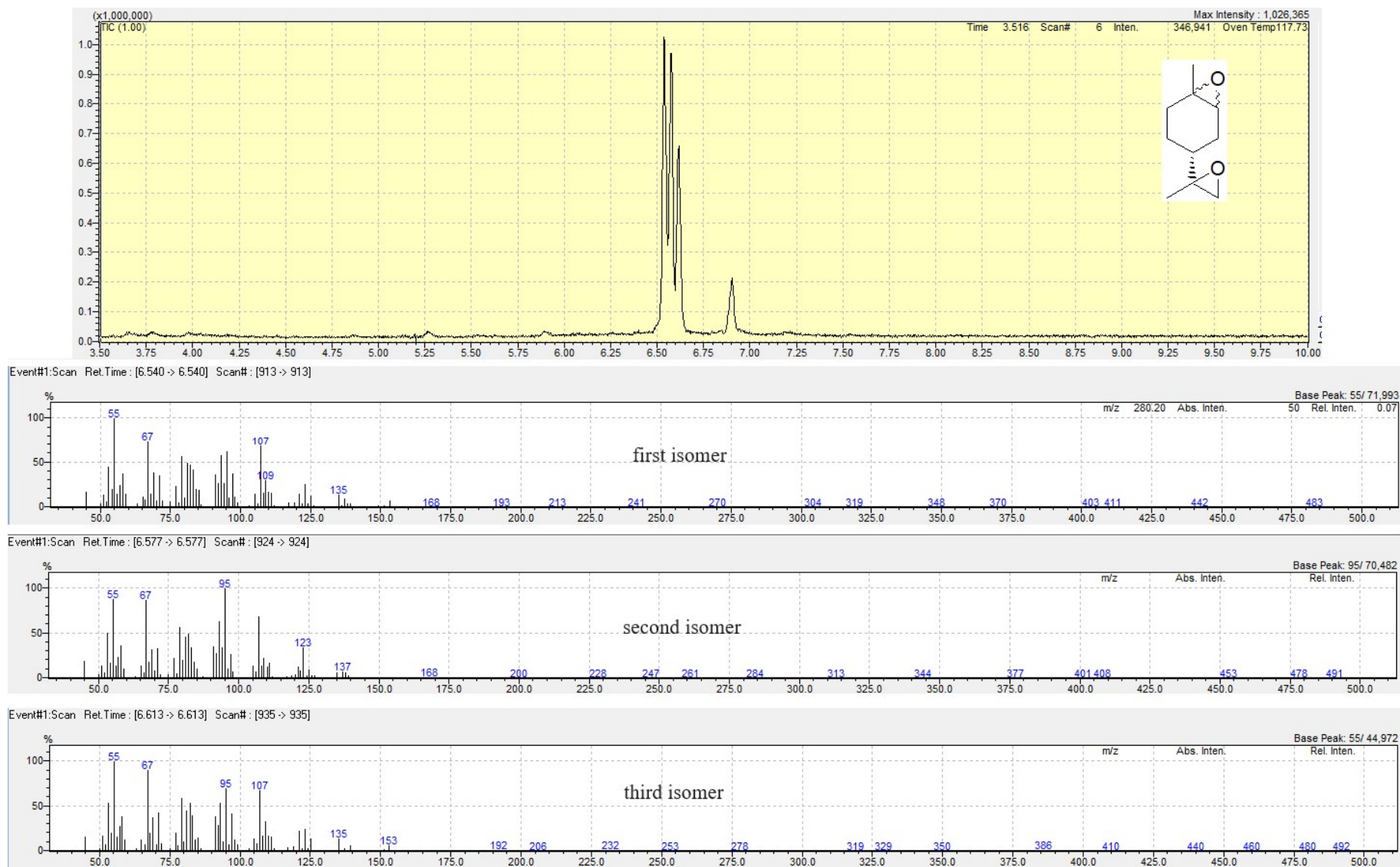


Figure S22. GC-MS of crude limonene diepoxide obtained from commercial (+)-limonene epoxide